Field emission properties of one-dimensional single CuO nanoneedle by in situ microscopy

**Yueli Liu · Lei Zhong · Zhuoyin Peng ·
Yanbao Song · Wen Chen**

Abstract In this article, the field-emission property of individual CuO nanoneedle was investigated to explore its tip image and real work function using in situ transmission electron microscopy. The maximum emission current of nanoneedle used in this study was 1.08 μA, and two different slopes in the corresponding F–N graph existed with work functions of the CuO nanoneedle being 1.12 and 0.58 eV. In comparison with the single CuO nanoneedle, the field enhancement β and parameter s of the CuO nanoneedle's film arrays were also studied, which showed that the screening effect played a key role in the field-emission process.

Introduction

With the needle-like tip, 1D CuO nanoneedles have a high aspect ratio of length to radius, and their high field enhancement factor achieves low turn-on voltage and high emission current, which is desired for emitter applications [1–4]. However, most of the previous studies have been focused on the statistical properties of a large number of collective nanomaterials. While the structure of an individual nanoneedle may strongly affect its field-emission property, the research on the field emission of individual nano-objects begins to attract considerable attention [5–7].

Till now, many technical approaches have been explored to study the field-emission properties of the 1D nanostructures, such as conductive atomic force microscopy [8], nanoemitter by laser-weld nanoassembly [9], and so on. Recently, in situ transmission electron microscopy has been widely used to directly investigate the field-emission property of 1D nanomaterials, such as carbon nanotubes and ZnO nanowires [10–12]. However, there are few studies concerning the field-emission properties of the individual CuO nanoneedle, and its intrinsic physical characteristic still needs to be actually confirmed, especially the real work function, the field-emission mechanism, and so on.

In continuation of our previous study [13], we try here to investigate the field-emission properties of an individual CuO nanoneedle by in situ microscopy. For further understanding, the comparison between the field-emission properties of the single CuO nanoneedle and CuO nanoneedle's film arrays is also studied, which is used to investigate the influence of the screening effect during the emission process.

Y. Liu · L. Zhong · Z. Peng · Y. Song · W. Chen (✉)
State Key Laboratory of Advanced Technology for Materials Synthesis and Processing, School of Materials Science and Engineering, Wuhan University of Technology, Wuhan 430070, People's Republic of China
e-mail: chenw@whut.edu.cn

Y. Liu
CEA Grenoble, UMR 5819 CEA CNRS, DSM, DRFMC, SPrAM, LEMOH, 38054 Grenoble 9, France

Experimental

Synthesis process

Experimentally, the plated copper nanocrystalline was synthesized by pulse plating technique, and 1D CuO nanoneedles were thermally oxidized by heating the copper nanocrystalline at 700 °C with a rate of 5 °C/min, then

holding for 1 h in the air, and cooling to room temperature, as described in our previous study [13].

Characterization

The specimens for transmission electron microscopic observations were prepared by scraping the black-colored synthesized materials from the surface of the substrate, followed by sonication in ethanol solvent. A droplet was dispersed on a TEM micro-grid for TEM observation. The morphologies and microstructures of the plated layers and CuO nanoneedles were characterized using scanning electron microscope (SEM) (SIRION, FEI, Netherlands), transmission electron microscope (TEM) (JEM2010, JEOL, Japan), and X-ray diffractometer (XRD) (D8 Advanced XRD, Bruker AXS, Germany).

For in situ measurement, a special TEM specimen holder is built in a JEOL 2010 TEM operated under the vacuum of 10^{-7} Torr at room temperature, which is quite similar to the equipments used by others [10–12]. A tungsten needle etched electrochemically acts as the movable cathode, and the opposite gold panel is used as the anode electrode. The distance between the two electrodes can be adjusted from several hundreds to several tens of nanometers, and it is fixed to be 100 μm in the experiment under this study. An individual nanoneedle is mounted and fixed on the tungsten needle by a piezo-driven nanomanipulator equipped in SEM equipment, which is used to

carry out the measurements for field emission and work function, and the detailed measurement for the CuO nanoneedle's film arrays is introduced in our previous study with the inter-electrode distance of 100 μm [13].

Results and discussion

When the plated layers are thermally treated at the temperature 700 °C in the air, well-aligned and vertically grown CuO nanoneedles are obtained within the host materials with a lengths over 10 μm and root diameters of 25-35 nm, and the SEM image is shown in Fig. 1a. Pure CuO nanoneedles are collected by scraping the black synthesized materials from the surface of the substrate, and the corresponding XRD pattern using Co target is shown in Fig. 1b. It is shown that only CuO phase (JCPDS No. 01-089-5895) exists without Cu_2O phase, which further confirms that the nanoneedles belongs to the CuO phase. In order to clarify their ordering crystal structures, the ideal HRTEM image is processed by inverse FFT via selecting only the matrix reflections from the ideal CuO structure, as shown in the inset of Fig. 1c. It shows that the nanoneedle exhibits the straight lattice fringes normal to the nanoneedle axis with a d-spacing of 0.253 nm, which is similar to the d-value of monocline CuO {001} crystal planes, which is also coincident with the XRD result in Fig. 1b.

Fig. 1 Typical microstructure characteristic of the as-grown CuO nanoneedles: a SEM image; b XRD pattern; and c HRTEM image (ideal HRTEM image inserted)
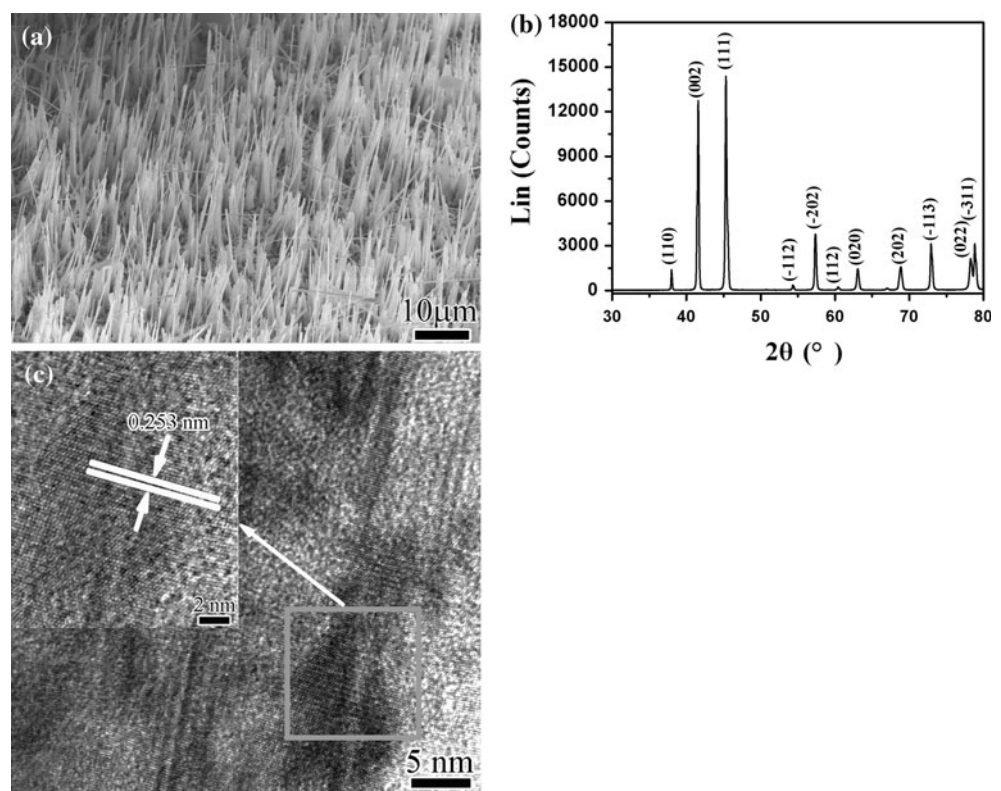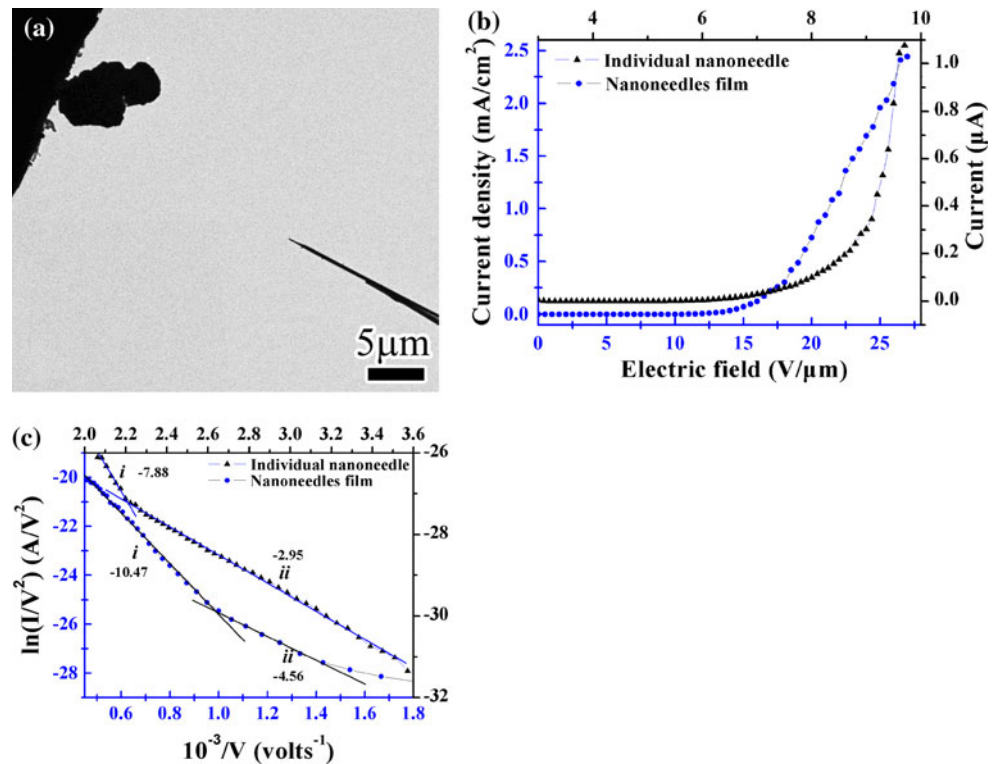
Fig. 2 Field emission measurements by in situ transmission electron microscopy: **a** in situ tip image; **b** I–V curve of the single CuO nanoneedle and CuO nanoneedle's film; and **c** the corresponding F–N graph of the single CuO nanoneedle and CuO nanoneedle's film

The free standing CuO nanoneedle is observed in *in-situ* TEM method, which exhibits a sharp tip structure with the tip diameter of 20 nm, as shown in Fig. 2a. The I–V curve and its corresponding F–N graph of single CuO nanoneedles and CuO nanoneedle's film arrays are shown in Fig. 2b and c, and Table 1 reveals the corresponding summarization for the structure parameters and the field emission properties of the 1D CuO single nanoneedle and nanoneedle's film arrays. The turn-on field (E_{to}) of the single CuO nanoneedle is about 5.3 V/μm at a current of 1 nA. The emission current increases exponentially with increasing inter-electrode voltage, and its maximum field-emission current is 1.08 μA when the electron emission filed is achieved at 9.70 V/μm. It shows that the emission current of the present CuO nanoneedles is quite high when compared with the others results, such as 6.0 nA of single CuO nanowire [8] and 0.80 μA of individual $W_{18}O_{49}$ nanowire [9], which implies that it may act as a good filed emitter.

When many cylindrical cathodes are brought together, a neighborhood screening effect appears and the local field on every tip decreases sharply with decreasing the distance between the nearest neighbors [6, 14–16]. In the model of "nanotube in conductive well" [6], it is shown that, from the view of the field-emission point, the real density of the nanostructure film is not so important: the extraction field can be attained at low anode voltage only on the highest tubes protruding from the average film structure. Therefore, the density of these higher tubes (usually called

Table 1 Structure parameters and FE properties of CuO single nanoneedle and nanoneedle's film

Parameters	CuO single nanoneedle	CuO nanoneedle's film
Height (h)	18 μm	15 μm
Radius (r)	10 nm	15 nm
Turn-on field (E_{to})	5.3 V/μm for 1 nA	0.5 V/μm for 10 μA/cm
Max current	1.08 μA at 9.7 V/μm	2.5 mA/cm² at 27 V/μm
Work function (φ)		
Low-field region	0.58 eV	0.58 eV
High-field region	1.12 eV	1.12 eV
Field enhancement (β)		
Low-field region	1021	661
High-field region		769
Field enhancement predicated (β)	None	6668
Screening effect (s)		
Low-field region	None	0.0989
High-field region		0.1153

emission site density (ESD)) is always used to character the effective density of CuO film to favor for the filed emission, and it is obviously of several orders of magnitude smaller than the film's real density. The maximum emission current density of CuO nanoneedles film arrays

shown in Fig. 1b is of 2.5 mA/cm^2 [13], then the ESD of the CuO film is estimated to be 2315 per cm^2 by considering the emission current of 1.08 μA for every single CuO nanoneedle.

It is well known that the F–N relationship can be simply expressed by such an equation as follows:

$$J = 1.54 \times 10^{-6} \frac{F^2}{\varphi} \exp{-6.83 \times 10^7 \frac{\varphi^{3/2}}{F}} \qquad (1)$$

where J is the emission current density (A/cm^2), F is the local field intensity (V/cm), and φ is the work function of emitters (eV).

The concept of field enhancement factor is defined by the following formula:

$$\beta = \frac{Fd}{V} \qquad (2)$$

where V is applied field voltage, and d is the distance between the anode and cathode; then the slope of measured $\ln(J/V^2)$ versus $1/V$ graph can be expressed as

$$k = \frac{-6.83 \times 10^7 d\varphi^{3/2}}{\beta} \qquad (3)$$

Then, the field-enhancement factor β and work function φ can be calculated according the Eq. 3. Normally, β is used to indicate the degree of the field-emission enhancement of any tip shape on a planar surface, which is a parameter depending on the nanoneedles' geometry, crystal structure, and the density of the emitting points.

The Fowler–Nordheim (F–N) graph of $\ln(J/V^2)$ against $1/V$ for the single CuO nanoneedle is shown in the upper line of Fig. 2c, and F–N graph of the CuO nanoneedle's film arrays in Fig. 2c in our previous study is also listed for clear comparative study [12]. The linear line indicates that the field-emission behavior follows the F–N mechanism where the electrons may tunnel through the potential barrier from conduction band (CB) to a vacuum state. It is worth pointing out that two slopes are found at the low- and high-field regions in F–N graphs of the single CuO nanoneedle and CuO nanoneedles film. These two slopes found in the F–N graphs can be attributed to the semiconductor feature of nanoneedles of this study where the electrons emitted from the nanoneedles may originate from two successive processes: the excitation of electrons from the valance band (VB) to the CB, and the emission from the CB to the vacuum state [17]. At low applied voltages, a few electrons can be excited from VB to CB and emitted from the nanoneedles. When the applied voltage is increased to a critical value, all electrons can be totally excited from the VB to the CB, exhibiting the quasimetallic behavior that can result in the increased β value in the high-field region [17]. Moreover, for single CuO nanoneedle, the joule heating effect under the high electric field may increase the

slope of the F–N curve [18]; for CuO nanoneedle film arrays, under high electric field. their characters with low height or smaller aspect ratio may start to emit electron, which can also increase the slope of the F–N curve [6].

Based on both of the experimental and simulated results, it was shown that the overall field enhancement of the various elements of a cathode can be pressed as a product of their respective field enhancement factors [19, 20]:

$$\beta = 1.2\left(\frac{h}{r} + 2.15\right)^{0.9} \times \left[1 + 0.013\frac{d}{d-h} - 0.033\frac{d-h}{d}\right] \qquad (4)$$

By taking h as 18 μm and r_{tip} of 10 nm from the TEM image in Fig. 2a, the present field enhancement β_{needle} of the singe CuO nanoneedle is observed to be 1021. Then combining with Eq. 3, the work function φ of the single CuO nanoneedle is calculated to be 1.12 and 0.58 eV in the slope (i) and (ii) at the high- and low-field regions in F–N graphs, respectively. This result is quite smaller than that of the bulk CuO work function [21]; however, it is in agreement with the range of our previous results [13] and the value of 0.3–2.62 eV reported by Chien and coworkers [1]. Moreover, choosing d as 100 μm in Eq. 3, the field enhancement β of the CuO nanoneedle's film arrays in Fig. 2c is also calculated to be 769 and 661 at the high- and low-field regions in F–N graphs, respectively.

As several emitters may be assembled to form a multiple source, screening effect between the emitters becomes significant even for large inter-needle distances [6]. By considering the screening effect, the following phenomenological formula is proposed for the strength of the electric field on the nanoneedle belonging to a cathode film whose average gap to the anode is d by Filip's model [6]:

$$F = s\frac{V}{r} + (1-s)\frac{V}{d} \qquad (5)$$

Obviously, the screening effect is entirely embedded in the parameter s, whose range is between 0 (for very densely arranged and uniformly oriented needles) and 1 (for a single nanoneedle). Combining the Eqs. 2 and 5, a formula to estimate the field enhancement factor of the emitter films β_{film} can be derived as follows:

$$\beta = 1 + s\left(\frac{d}{r} - 1\right) \cong 1 + s\frac{d}{r} \qquad (6)$$

From the above equation, it should be concluded that, in practice, the parameter β is not a characteristic of the nanoneedle's film but of the entire setup for a film, as it depends on the gap distance d. Therefore, the screening effect is entirely embedded in the parameter s. Defining s as 1 for a single CuO nanoneedle in the film formation and the average tip diameter of 15 nm, the field enhancement of the single CuO nanoneedles in film formation $\beta_{nanoneedle}$

is to be 6668 when the value of the distance d is 100 μm. On the other hand, using the actual β value from field-emission measurements, the parameter s is estimated to be 0.1153 and 0.0989 at the high- and low-field regions in F–N graphs, respectively, which implies that the screening effect plays an important role in the actual field-emission process from nanoneedle's arrays. This can also be seen from the SEM image shown in Fig. 1a, in which the CuO nanoneedles with high density cover a large area of the substrate, resulting in the domination of the screening effect. It is expected that the field-emission properties will be greatly improved by using CuO nanoneedle's arrays with lower growth density [22].

For the case of film-like materials, the parameters determining the field amplification includes the emitters' height h and their inter-distance l in the model of "nanotube in conductive well" [6], as the height h is also significant even for several micrometer long needles as proven by electrostatic calculations, and the screening between the emitters become significant even for large inter-emitter distances l [7]. Therefore, by taking the film's morphology into account, the field enhancement of the CuO nanoneedle's film arrays β_{film} should be estimated, such as the height h and inter-needle distance l [5–7]. Then, a function is extracted from the following calculation:

$$\beta_{film}(l, h, r) = \beta_{nanoneedle} f(lh_0/h)$$
$$= \beta_{nanoneedle}(1 - \exp(-1.1586 lh_0/h)) \quad (7)$$

In the above equation, h_0 is confirmed to be 2.0 μm. Assuming the l as 1.0 μm (the corresponding density of the film is 10^8 per cm^2), the even height h as 22 μm, and $\beta_{nanoneedle}$ as 6668, then the field enhancement β_{film} is calculated to be 667, which is quite similar to the experimental value of 661 at low-field regions, and much deviating from the value of the 769 at high-field regions mentioned above; it is due to the fact that the nanoneedles with lower height or smaller aspect ratio may start to emit electron under high electric field [6]. This fact implies that the inter-needle distance d should be much over 1.0 μm due to the higher screening effect at the high-field region, which also confirms that the screening effect plays a quite important role in the field-emission property.

Conclusion

In conclusion, the field emission of an individual nanoneedle possesses good field-emission properties, such as low turn-on field of 5.3 V/μm, high maximum current of 1.08 μA at 9.7 V/μm, and linear F–N graph, indicating that the present CuO nanoneedle would be a good potential application in field-emission area. Two different slopes appear in the corresponding F–N graph, which represents

that the work function of the present CuO nanoneedle is to be 1.12 and 0.58 eV at high- and low-field regions, respectively. At the same time, the field enhancement β of the CuO nanoneedle's film is calculated to be 769 and 661, and their corresponding parameter s for screening effect is 0.1153 and 0.0989, respectively. The results showed that the screening effect played a key role in the field-emission properties.

References

1. Hsieha C-T, Chen J-M, Lin H-H, Shih H-C (2003) App Phys Lett 83(16):3383
2. Chen J, Deng SZ, She JC, Xu NS, Zhang WX, Wen XG, Yang SH (2003) J Appl Phys 93(3):1774
3. Chen US, Chueh YL, Lai SH, Chou LJ, Shih HC (2006) J Vac Sci Technol B 24(10):139
4. Gandhi S, Subramani RHH, Ramakrishnan T, Sivabalan A, Dhanalakshmi V, Nair MRG, Anbarasan R (2010) J Mater Sci 45(6):1688. doi:10.1007/s10853-009-4158-4
5. Zhu YW, Yu T, Cheong FC, Xu XJ, Lim CT, Tan VBC, Thong JTL, Sow CH (2005) Nanotechnology 16:88
6. Filip V, Nicolaescu D, Tanemura M, Okuyama F (2001) Ultramicroscopy 89:39
7. Bonard J-M, Weiss N, Kind H, Stőckli T, Forró L, Kern K, Châtelain A (2001) Adv Mater 13(3):184
8. Cheng G, Wang SJ, Cheng K, Jiang XH, Wang LX, Li LS, Du ZL, Zou GT (2008) Appl Phys Lett 92:223116
9. She JC, An S, Deng SZ, Chen J, Xiao ZM, Zhou J, Xu NS (2007) Appl Phys Lett 90:073130
10. Xu Z, Bai XD, Wang EG, Wang ZL (2005) Appl Phys Lett 87:163106
11. Wang ZL, Gao RP, de Heer WA, Poncharal P (2002) Appl Phys Lett 80:856
12. Wang ZL, Poncharal P, de Heer WA (2000) Microsc Microanal 6:224
13. Liu YL, Liao L, Li JC, Pan CX (2007) J Phys Chem C 111:5050
14. Nicolaescu D, Filip V, Wilshaw PR (1996) Appl Surf Sci 94–95:79
15. Nilsson L, Groening O, Emmenegger C, Kuettel O, Schaller E, Schlapbach L, Kind H, Bonard J-M, Kern K (2000) Appl Phys Lett 76:2071
16. Groning O, Kuttel OM, Emmenegger C, Groning P, Schlapbach L (2000) J Vac Sci Technol B 18:665
17. Chueh YL, Lai MW, Liang JQ, Chou LJ, Wang ZL (2006) Adv Funct Mater 16(17):2243
18. Peng XL (2000) Thin Solid Films 372:292

19. Boratd JM, Dean KA, Coll BF, Klinke C (2002) Phys Rev Lett 89:197602

20. Kim CD, Jang HS, Lee SY, Lee HR, Roh YS, Rhee IS, Lee EW, Yang HS, Kim DH (2006) Nanotechnology 17(20):5180

21. Seelaboyina R, Huang J, Park J, Kang DH, Choi WB (2006) Nanotechnology 17:4840

22. Zhao Q, Xu J, Xu XY, Wang Z, Yu DP (2004) Appl Phys Lett 85(22):5331